Repulsive Casimir forces with finite-thickness slabs

R. Zhao,[1,2] Th. Koschny,[1,3] E. N. Economou,[3] and C. M. Soukoulis[1,3]

[1]*Ames Laboratory and Department of Physics and Astronomy, Iowa State University, Ames, Iowa 50011, USA*

[2]*Applied Optics Beijing Area Major Laboratory, Department of Physics, Beijing Normal University, Beijing 100875, China*

[3]*Institute of Electronic Structure and Laser, FORTH, Department of Materials Science and Technology, University of Crete, Heraklion, G-71110 Crete, Greece*

(Received 3 July 2010; revised manuscript received 17 November 2010; published 9 February 2011)

We use the extended Lifshitz theory to study the behaviors of the Casimir forces between finite-thickness effective medium slabs. We first study the interaction between a semi-infinite Drude metal and a finite-thickness magnetic slab with or without substrate. For no substrate, the large distance d dependence of the force is repulsive and goes as $1/d^5$; for the Drude metal substrate, a stable equilibrium point appears at an intermediate distance that can be tuned by the thickness of the slab. We then study the interaction between two identical chiral metamaterial slabs, with and without substrate. For no substrate, the finite thickness of the slabs D does not significantly influence the repulsive character of the force at short distances, while the attractive character at large distances becomes weaker and behaves as $1/d^6$; for the Drude metal substrate, the finite thickness of the slabs D does not influence the repulsive force too much at short distances until $D = 0.05\lambda_0$.

DOI: 10.1103/PhysRevB.83.075108 PACS number(s): 12.20.−m, 41.20.Jb, 81.05.Xj, 78.67.Pt

I. INTRODUCTION

Arising from the quantum fluctuations of the vacuum field, when two neutral parallel conducting surfaces separated by the vacuum are very close to each other, they generate an attractive force between them given by $F = -\frac{\hbar c \pi^2 A}{240 d^4}$ and called *Casimir force* after the founder Casimir.[1] The Casimir force becomes more pronounced if the dimension goes to nanoscale. It will lead to stiction and adhesion on the surface,[2,3] which is a challenge for flexibly operating the micro-/nanoelectromechanical system devices. Later, especially recently, people were(are) pursuing different methods to control the Casimir force so as to obtain a repulsive force: immersing two objects characterized by the dielectric permittivities $\epsilon_1(i\xi)$ and $\epsilon_2(i\xi)$ in a fluid with $\epsilon_3(i\xi)$ [satisfying $\epsilon_1(i\xi) < \epsilon_3(i\xi) < \epsilon_2(i\xi)$],[4,5] using a special geometry,[6] an electric ($\epsilon > \mu$) plate together with a magnetic ($\mu > \epsilon$) plate,[7,8] two interacting plates sandwiching a perfect lens,[9] and resorting to strong chirality materials.[10,11] Only for the first two proposals can natural materials be utilized; for the others, they all need some exotic materials, that is, strong magnetodielectric response materials,[12–14] perfect lens,[9] and strong chiral metamaterials (CMMs).[10,11] These materials do not exist in nature and can only potentially be made artificially. This type of material is called *metamaterial*.[15] Under current technologies, the thickness of these metamaterials cannot be made very large, especially at the optical regime.[16,17] The thickest optical negative index metamaterial so far is only about half of the operating wavelength.[18] What we can obtain is just a finite-thickness artificial metamaterial slab with or without a substrate. Therefore, in this paper, we study the behaviors of the repulsive Casimir forces with finite-thickness effective medium slabs for two of the aforementioned proposals: with strong magnetodielectric response materials[12–14] and with strong CMMs.[10,11]

First, we briefly introduce the extended Lifshitz theory, which is valid for CMMs as well. Lifshitz[19] generalized the calculation of Casimir force between two semi-infinite planar and parallel objects, 1 and 2, characterized by frequency-dependent dielectric functions $\epsilon_1(\omega)$ and $\epsilon_2(\omega)$. Later there was further extension to general bi-anisotropic media.[20–22] The formula for the force or the interaction energy per unit area can be expressed in terms of the reflection amplitudes r_j^{ab} $(j = 1,2)$,[23] at the interface between the vacuum and the object j, giving the ratio of the reflected electromagnetic wave of polarization a by the incoming wave of polarization b. Each a and b stands for either electric (TM or p) or magnetic (TE or s) waves. The frequency integration is performed along the imaginary axis by setting $\omega = i\xi$. The interaction energy per unit area is given by

$$\frac{E(d)}{A} = \frac{\hbar}{2\pi}\int_0^{+\infty} d\xi \int \frac{d^2\mathbf{k}_\parallel}{(2\pi)^2} \ln\det \mathbf{G}, \tag{1}$$

where $\mathbf{G} = 1 - \mathbf{R}_1 \cdot \mathbf{R}_2 e^{-2K_0 d}$,

$$\mathbf{R}_j = \begin{vmatrix} r_j^{ss} & r_j^{sp} \\ r_j^{ps} & r_j^{pp} \end{vmatrix}, \tag{2}$$

and $K_0 = \sqrt{\mathbf{k}_\parallel^2 + \epsilon_0\mu_0\xi^2}$; ϵ_0 and μ_0 are the permittivity and permeability of free space, and d is the distance between the two interacting plates. A negative(positive) slope of $E(d)$ corresponds to a repulsive(attractive) force.

For a finite-thickness isotropic achiral slab j with a semi-infinite isotropic achiral substrate medium j', the reflection elements are the results of the multiscattering by the finite slab and written as

$$r_j^{ab} = \frac{r_{0j}^{ab} + r_{jj'}^{ab} e^{-2K_j d_j}}{1 + r_{0j}^{ab} r_{jj'}^{ab} e^{-2K_j d_j}}, \tag{3}$$

where d_j is the thickness of the slab j, $K_j = \sqrt{\mathbf{k}_\parallel^2 + \epsilon_0\mu_0\epsilon_{rj}\mu_{rj}\xi^2}$, and ϵ_{rj} and μ_{rj} are the relative permittivity and permeability of the medium j. In r_{mn}^{ab}, superscripts a and b are defined the same way as in Eq. (2) and subscripts m and n denote that the light is incident from the medium m

 ©2011 American Physical Society

to n. 0 means vacuum. r_{mn}^{ab} are given as[24]

$$r_{mn}^{ss} = (\mu_{rn}K_m - \mu_{rm}K_n)/(\mu_{rn}K_m + \mu_{rm}K_n), \quad (4a)$$

$$r_{mn}^{pp} = (\epsilon_{rn}K_m - \epsilon_{rm}K_n)/(\epsilon_{rn}K_m + \epsilon_{rm}K_n), \quad (4b)$$

$$r_{mn}^{sp} = r_{mn}^{ps} = 0. \quad (4c)$$

For a finite-thickness isotropic chiral slab j with a semi-infinite isotropic achiral substrate medium j', the nondiagonal terms, r^{sp} and r^{ps}, are nonzero. The total reflection matrix can be written as[25]

$$\mathbf{R}_j = \mathbf{R}_{0j} + \mathbf{T}_{j0}\mathbf{\Delta}_j\mathbf{R}_{jj'}\mathbf{\Delta}_j[\mathbf{I} - \mathbf{R}_{j0}\mathbf{\Delta}_j\mathbf{R}_{jj'}\mathbf{\Delta}_j]^{-1}\mathbf{T}_{0j}, \quad (5)$$

where $\mathbf{I}$ is the unit matrix and

$$\mathbf{\Delta}_j = \begin{vmatrix} e^{-K_{j+}d_j} & 0 \\ 0 & e^{-K_{j-}d_j} \end{vmatrix}, \quad (6)$$

where $K_{j\pm} = \sqrt{\mathbf{k}_\parallel^2 + n_{j\pm}^2(i\xi)\xi^2/c^2}$ and $n_{j\pm}(i\xi) = \sqrt{\epsilon_{rj}(i\xi)\mu_{rj}(i\xi)} \pm \kappa_j(i\xi)$. $\epsilon_{rj}(i\xi)$ and $\mu_{rj}(i\xi)$ are the relative permittivity and permeability of the chiral slab j, respectively, and $\kappa_j(i\xi)$ is the chirality coefficient; c is the velocity of the light in vacuum. Matrices $\mathbf{R}_{mn}$ and $\mathbf{T}_{mn}$ are the reflection and transmission matrices at the interface of the medium m and n. The subscripts m and n still denote that the incident light is from the medium m to n. The detailed expressions of these matrices' elements can be found in Ref. 26.

II. REPULSIVE CASIMIR FORCES WITH MAGNETIC SLABS

There are claims, for example, in Ref. 27, that when metamaterials are made of ordinary materials with a negligible intrinsic magnetic response, repulsion is impossible at large distances, but this does not deny the possibility that a paramagnetic slab and a dielectric slab repel each other. Yannopapas and his collaborator recently resorted to the magnetic response of paramagnetic composites and theoretically obtained a repulsive Casimir force in the micrometer scale.[14] Therefore, by employing a proper magnetic response, it is still possible to get a repulsive force. Here we characterize the electric and magnetic response as

$$\epsilon(i\xi) = 1 + \frac{\Omega_\epsilon\omega_\epsilon^2}{\xi^2 + \omega_\epsilon^2 + \gamma_\epsilon\xi}, \quad (7a)$$

$$\mu(i\xi) = 1 + \frac{\Omega_\mu\omega_\mu^2}{\xi^2 + \omega_\mu^2 + \gamma_\mu\xi}, \quad (7b)$$

where Ω_ϵ and Ω_μ denote the strengths of the electric permittivity and magnetic permeability, ω_ϵ and ω_μ are the electric and magnetic resonance frequencies, and γ_ϵ and γ_μ are the collision frequencies. However, note that a ξ dependence of μ as in Eq. (7b) is questionable, since in the existing calculations one obtains that the constant Ω_μ is actually replaced by $\Omega_\mu\xi^2$, and the 1 by $1 - \Omega_\mu\omega_\mu^2$; the latter because $\mu(+\infty) \to 1$. The magnetic response shown in (7b) is assumed to come from the parallel alignment of very small ferromagnetic nanoparticles in an applied magnetic field; therefore, the magnetic resonance frequency is expected to be lower than the electric one. We choose the parameters $\omega_\epsilon = 10\omega_0$, $\omega_\mu = \omega_0$, and $\gamma_\epsilon = \gamma_\mu = 0.05\omega_0$, where ω_0 is the normalized frequency. To get a repulsive force, the inequality $\Omega_\mu > \Omega_\epsilon$ should be satisfied. Here, we choose $\Omega_\mu = 2$ and $\Omega_\epsilon = 1$ as an example. In the following, we calculate the Casimir force between a semi-infinite Drude metal plate, characterized by $\epsilon(i\xi) = 1 + \omega_{pl}^2/(\xi^2 + \xi\gamma_{pl})$, with $\omega_{pl} = 100\omega_0$ and $\gamma_{pl} = 0.05\omega_0$, and a magnetic slab of finite thickness $d_2 \equiv D$. Two cases are studied in this paper: (i) with no substrate, as shown in the inset in Fig. 1(b); and (ii) with a semi-infinite Drude metal substate as shown by the inset in Fig. 1(d).

A. No substrate

Figures 1(a) and 1(b) show the Casimir interaction energy per unit area E/A versus k_0d between a semi-infinite Drude metal plate and a finite-thickness magnetic slab with no substrate. Different curves correspond to different values of the thickness D of the slab. $k_0 = 2\pi/\lambda_0$ and $\lambda_0 = 2\pi c/\omega_0$. These figures show that the Casimir energies exhibit a similar behavior for slabs of different thicknesses (from $D = +\infty$ to $D = 0.01\lambda_0$). Indeed, all Casimir energy curves exhibit a repulsive character for large distances and an attractive one for small distances. Thus, there is only one energy peak (indicating an unstable equilibrium point), appearing approximately at $k_0d \simeq 0.7$ for all thickness D; the strength of this peak is diminishing as the thickness becomes smaller (especially for $D < 0.1\lambda_0$). Figure 1(b) shows that, at large distances, the d dependence of the Casimir energy changes from $1/d^3$ (for infinite thickness, $D = +\infty$) to $1/d^4$ (for $D = 0.01\lambda_0$); the $1/d^3$ dependence is typical for semi-infinite slabs. Similar d dependence was also found between ordinary media.[28] At small distances, all the Casimir energy curves for different values of thickness (from $D = +\infty$ to $D = 0.1\lambda_0$) in Fig. 1(a) overlap very well. As shown in Fig. 1(b), note that for $D = 10\lambda_0$, the energy curve overlaps with the $D = +\infty$ below $k_0d = 10$. If the thickness D becomes smaller, $D = 0.1\lambda_0$, the different energy curves overlap below $k_0d = 0.1$.

B. Drude metal substrate

Figures 1(c) and 1(d) show the Casimir interaction energy per unit area E/A versus k_0d between a semi-infinite Drude metal plate and a finite magnetic slab with a semi-infinite Drude metal substrate. Different curves correspond to different values of the thickness D of the slab. These figures show that the behaviors of the Casimir interaction energies are different for different thicknesses of the slabs. If the finite magnetic slab is very thin (e.g., $D \leqslant 0.1\lambda_0$ in our case), the Casimir force is attractive for any distance. A very interesting behavior appears for large (but finite) thicknesses ($D \geqslant \lambda_0$ in our case): At very large distances d the interaction is attractive (the interaction energy is negative and decreasing with decreasing d). Figure 1(d) shows that at large distances the d dependence of Casimir energy is $1/d^3$ and does not change with the thickness of the slab. At some distance d_s ($k_0d_s \simeq 10$ for $D = \lambda_0$ and $k_0d_s \simeq 10^2$ for $D = 10\lambda_0$) the interaction energy reaches a local minimum (indicating a stable equilibrium distance), and then the curve increases as d decreases, it crosses the axis at some point d_0 ($d_0 < d_s$), and it reaches a maximum at $d = d_u$ (at d_u we have an unstable equilibrium distance); d_u seems to be about the same for all thicknesses $D \geqslant \lambda_0$. For $d < d_u$

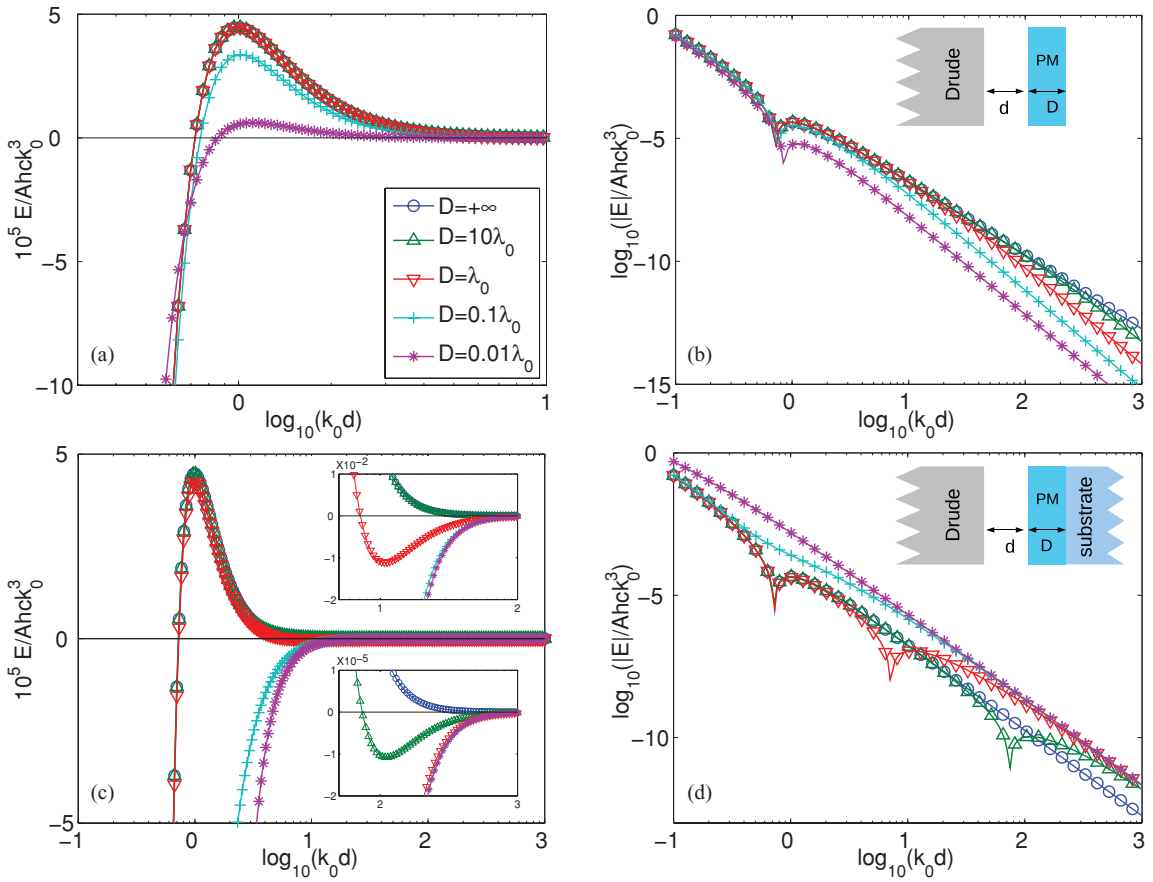

FIG. 1. (Color online) Casimir interaction energy per unit area $E(d)/A$ (in units of hck_0^3) versus k_0d between a semi-infinite Drude metal plate and a finite magnetic slab (a,b) without substrate and (c,d) with Drude metal substrate. (b,d) Insets: schematics depicting the arrangements of the slabs or substrates. Curves correspond to different values of the thickness D of the slab. (a,c) Linear-log plot; (b,d) log-log plot. (c) Insets: magnifications of the regions around $k_0d \simeq 10$ and $k_0d \simeq 10^2$.

the energy curve decreases with decreasing d (indicating an attractive Casimir force) and crosses the axis at a distance d_0', which seems to be common for all $D \geqslant \lambda_0$. The points d_0 and d_0' are shown as sharp dips in the log-log plot [Fig. 1(d)]. It seems that d_0 and d_s tend to infinity as $D \to +\infty$.

The appearance of an equilibrium point at the distance $d = d_s$ is of great importance: first, because it can be tuned by the thickness D; second, because its magnitude can be larger than the wavelength and/or the size of the unit cell of the magnetic metamaterial, and consequently, it is in the range of validity of the effective medium approximation (EFA) on which Eqs. (1)–(7b) are based ($d \geqslant \lambda_0, D$), for example, for $\lambda_0 = 700$ nm and $D = 7\ \mu$m, $d_s \simeq 1\ \mu$m.

III. REPULSIVE CASIMIR FORCES WITH CHIRAL SLABS

Repulsive Casimir force was also found to be realized by using CMMs if the chirality is strong enough.[10,11] Here, we study the repulsive Casimir force between two finite-thickness CMM slabs, with and without the Drude metal substrate. The optical parameters of CMMs are characterized by[11]

$$\epsilon(i\xi) = 1 + \frac{\Omega_\epsilon \omega_\epsilon^2}{\xi^2 + \omega_\epsilon^2 + \gamma_\epsilon \xi}, \tag{8a}$$

$$\mu(i\xi) = 1 + \Omega_\mu - \frac{\Omega_\mu \xi^2}{\xi^2 + \omega_\mu^2 + \gamma_\mu \xi}, \tag{8b}$$

$$\kappa(i\xi) = \frac{i\Omega_\kappa \xi}{\xi^2 + \omega_\kappa^2 + \gamma_\kappa \xi}, \tag{8c}$$

where Ω_κ denotes the strength of the chirality resonance, ω_κ is the resonance frequency of chiral structure, and γ_κ is the collision frequency. Usually, the electric, magnetic, and chirality resonances are at the same frequency, therefore, we set $\omega_\epsilon = \omega_\mu = \omega_\kappa = \omega_0$ and $\gamma_\epsilon = \gamma_\mu = \gamma_\kappa = 0.05\omega_0$. To get a repulsive force, Ω_κ should be large enough. Here, $\Omega_\epsilon = 1$, $\Omega_\mu = 0.001$, and $\Omega_\kappa = 0.7$, that is, large enough for repulsive forces to appear. The two slabs are identical with the same parameters and substrate as shown by the insets in Figs. 2(b) and 2(d). Then we still consider two cases: (i) with no substrate, as shown by the inset in Fig. 2(b); and (ii) with semi-infinite Drude metal substate as shown by the inset in Fig. 2(d).

A. No substrate

Figures 2(a) and 2(b) show the Casimir interaction energy between two finite chiral slabs without substrate. Different curves correspond to different values of the thickness D of the slabs. We see that no matter how thin (from $+\infty$ to $0.01\lambda_0$) the

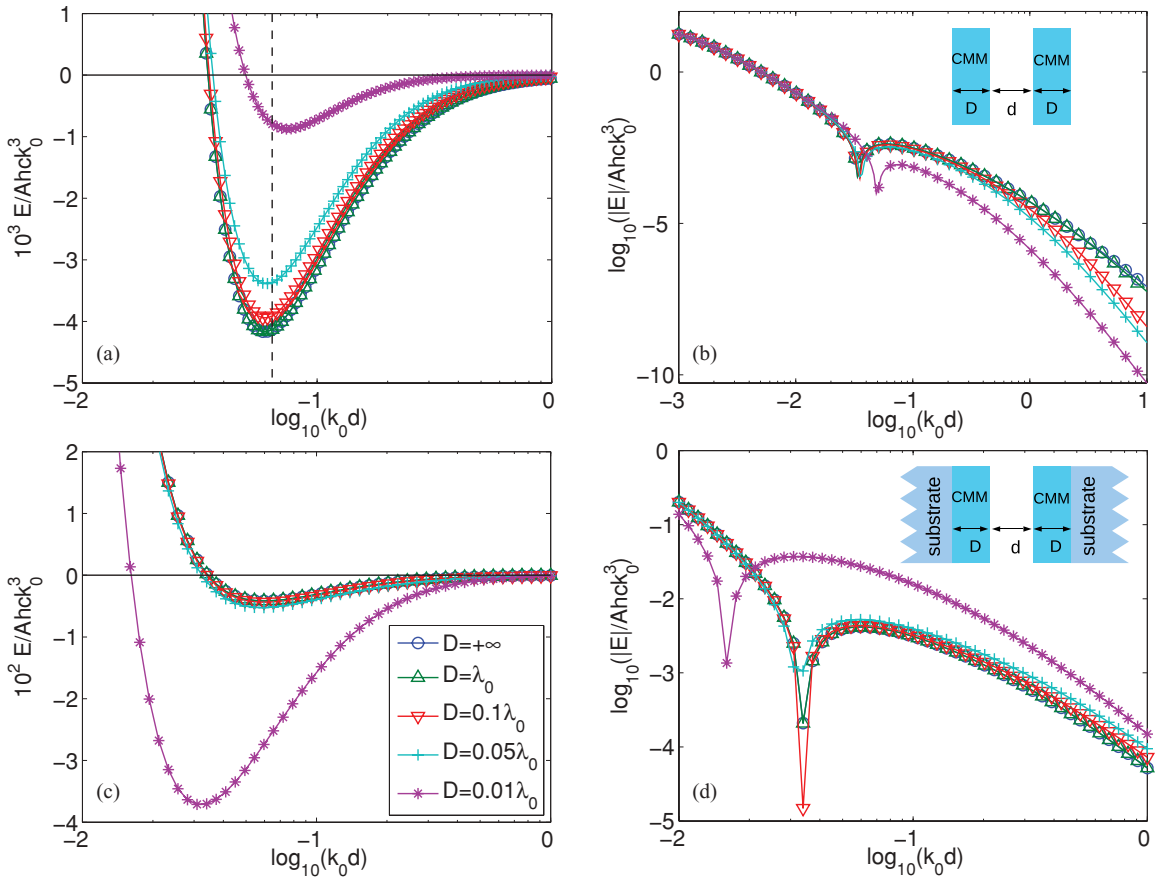

FIG. 2. (Color online) Casimir interaction energy per unit area $E(d)/A$ (in units of hck_0^3) versus k_0d between two identical finite-thickness CMM slabs (a,b) without substrate and (c,d) with semi-infinite Drude metal substrate. (b,d) Insets: schematics depicting the arrangements of the slabs or substrates. Curves correspond to different values of the thickness D of the slab. (a,c) Linear-log plot; (b,d) log-log plot.

slabs are, there is only one energy minimum over the whole distance range (from $k_0d = 10^{-3}$ to 10); that is, in all cases, the Casimir forces have the same behavior—repulsive force at small distances and attractive force at large distances—as shown in Ref. 10. All the stable equilibrium points are at about $k_0d = 0.07$, where the force changes from attractive to repulsive. As the dashed vertical line at $k_0d = 0.064\,42$ shows, the minimum is at a slightly larger distance for small D. Note that the minimum appears at a very small distance d, which makes the validity of the effective medium theory (EMT) doubtful.[29] Figure 2(b) shows, similarly, that at large distances the d dependence of the Casimir energy for finite-thickness slabs is $1/d^5$, as opposed to the $1/d^3$ between two semi-infinite media. This d dependence was also found theoretically between ordinary slabs.[28] At small distances, all the Casimir energies for different thicknesses of the finite slabs tend to coincide. However, for such short distances, the EMT is expected to fail and the microstructure effect will dominate the Casimir repulsion effect.[29]

B. Drude metal substrate

Figures 2(c) and 2(d) show the Casimir interaction energy between two identical finite CMM slabs with the Drude metal substrate. It shows that the behaviors of the Casimir interaction energy are almost the same if the thickness of the slab is larger than $0.05\lambda_0$. Thinner slabs can still give us the repulsive force, but at a smaller distance, for example, for $D = 0.01\lambda_0$, a repulsive force appears when $k_0d < 0.035$. In other words, if we want to demonstrate the Casimir force experimentally, a $0.05\lambda_0$-thickness slab is enough to observe all the phenomena, assuming the validity of the EMT, which is doubtful for such short distances, and no microstructure effect.[29]

IV. DISCUSSION OF THE VALIDITY OF THE EFFECTIVE MEDIUM APPROXIMATION

Reference 29 presents a test of the EMA for CMMs (as also used in this present paper) against numerical calculations that include the microstructures. A numerical proof was presented[29] that the effective homogeneous approximation breaks down when the separation distance between the two plates becomes comparable to the size of the unit cell of the CMM making the two plates. On the contrary, we have shown here, and in our previous work,[10,11] that chirality makes a repulsive contribution to the Casimir force. Our proof[10,11] is based on the constitutive equations connecting the Maxwell vectors; these equations are definitely valid in the regime $a \ll t, a \ll d$, where a is the unit cell size of the CMM, t is the thickness of the plates, and d is the separation between the plates. By making a small enough, we can satisfy the double inequality $a \ll d \ll d_0$, where d_0 is a separation

distance, such that the Casimir force is appreciable including the chiral repulsive contribution to it. We have shown in the present paper that the combination of plates of finite thickness with appropriate background substantially facilitates the satisfaction of the double inequality. Thus we argue that, because the present article and Ref. 29 consider very different situations, there is no contradiction whatsoever between the two, as explained in detail below.

Previously it has been shown[10,11] that two semi-infinite, homogeneous, and isotropic chiral media separated by a finite-thickness vacuum slab will experience a repulsive Casimir force between one another—or at least a significant reduction of the attractive Casimir force—at small separations if the chirality of the embedding media becomes large enough. It has been speculated that such chiral materials could at least, in principle, be implemented by CMMs in the homogeneous effective medium limit (i.e., where the EMA is valid). The major contribution to the Casimir force comes from frequencies and wave vectors of order of magnitude comparable to that of the inverse separation of the chiral media; it is in this region at least where the implementation of the CMMs should allow EMA.

Now, from here chiral Casimir repulsion has been further investigated in at least two directions.

(i) Assume an existing CMM structure with a given unit cell size; the extent to which a repulsive contribution to the Casimir force can be found (in simulations) for a discreet metamaterial has been investigated . This is the topic of Ref. 29, where only a minimal repulsive contribution to the Casimir force was found at a separation much larger than the unit cell size of the metamaterial: a regime where also the repulsive contribution in the analytical calculation of homogeneous semi-infinite media would become negligible. Not surprisingly, for separations comparable in order of magnitude to the unit cell size of the metamaterial, it was determined that the discrete interactions between the constituents of the metamaterials dominate the force and no chiral repulsion could be observed because the metamaterials no longer behave as homogeneous media at the relevant frequencies and wave vectors. Theoretically, this problem could be easily corrected by just making sure the structural length scale, that is, the assumed unit cell size, is small compared to the separation maintaining the validity of the EMA at the relevant frequencies and wave vectors. Of course, in reality this could be a problem because there are current practical limits to the nanofabrication of the metamaterial structures (e.g., for repulsion at 1-μm separation the structural length scale of the metamaterial should be well below 100 nm to ensure homogeneous effective medium behavior). The effect of finite thickness was not studied in Ref. 29: the media were just chosen thick enough to behave as if they where in fact semi-infinite.

(ii) In this paper we follow a very different direction. We keep the assumptions of homogeneous isotropic chiral media and investigate the question how a finite thickness of the semi-infinite chiral media, terminated by air or metal, will affect the sign and magnitude of the Casimir force as well as its scaling with the separation between the media. We consider the homogeneity and isotropy of the chiral materials as given; hence, the implementation by any to-be-designed CMM as a technical problem that can be considered independently. We believe that this investigation provides valuable information about the physical interplay between Casimir repulsion and attraction brought about by these boundary conditions and is relevant, if an effectively homogeneous metamaterial implementation is fabricated. So, in summary, the present work and Ref. 29 do not contradict each other but shed light on the possibility of a repulsive or reduced-magnitude Casimir force from different angles.

We believe the approach taken and results presented here are independent of Ref. 29, not a mere extension of previous work,[10,11] and provide new results for finite-thickness effective medium slabs. The discussion of scaling of the Casimir force with separation for the different regimes of thin versus thick finite chiral media slabs, the observation of stable equilibrium points, and the discussion of the effects of different terminations/substrates are unique and important results presented here.

Finally, the research reported here is in no way "invalidated" by the results reported in Ref. 29. This previous publication[29] only asserts that once the separation between the chiral media implemented by CMMs becomes comparable to the structural length scale of the metamaterials, discrete interactions become dominant and the repulsive Casimir force component expected form homogeneous chiral media ceases to exist. Theoretically, the repulsive component to the Casimir force should still exist at any given separation between the chiral media, if only the structural length scale is chosen small enough to ensure validity of the EMA at the relevant frequencies and wave vectors as explained above.

V. EXPLANATION

Here, we give a physical explanation regarding the Casimir force behaviors shown above: For large distances, the main contribution to the Casimir force comes from the frequencies $\xi < c/d$.[12] Since c/d is small, the main contribution region comes from low frequencies. For the low-frequency waves, the finite thickness of the slab is much less than the wavelengths; therefore, the effective optical parameters of the slab/substrate approach those of the substrate. If the substrate is vacuum, the effective optical parameters of the finite slab approach those of the vacuum; therefore, the Casimir energy of the finite slab with no substrate decreases more rapidly than the traditional Casimir force between two semi-infinite media. Therefore, for the Casimir force between a semi-infinite Drude metal and a finite slab without substrate, the d dependence for large d is $1/d^5$; and for the Casimir force between two identical finite chiral slabs without substrate, the d dependence is $1/d^6$. This behavior of the d dependence is the same as that in ordinary slabs.[28] If the substrate is Drude metal, the effective optical parameters of the finite slab/substrate for large distances approach those of Drude metal; therefore, at very large distances, every force approaches that of the interaction between two semi-infinite Drude metal media, that is, it is always an attractive force at large distance. For short distances, c/d is large. The main contribution region will come from high frequencies (short wavelengths). The influence of the substrate on the finite slab will be small. Therefore, for short distances the slab/substrate system tends to behave as a semi-infinite slab. The interesting behavior appears

at intermediate distances for the Drude/magnetic slab/Drude system [see Figs. 1(c) and 1(d)], where the repulsive character of the Drude/slab subsystem competes with the attractive subsystem Drude/Drude. That is why the magnetic slab with a Drude metal substrate can give us the equilibrium point at the intermediate distance. We repeat that for short distances, c/d is large. Hence, the influence of the substrate on the finite slab will be small. Therefore, the finite slab can be considered as a semi-infinite object. As a result, every curve goes to the same value at very small distances. A similar conclusion was given in Ref. 30. An equilibrium point behavior similar to that shown in the inset in Fig. 1(c) can also be obtained between two dielectric slabs, $\epsilon_1(i\xi)$ and $\epsilon_2(i\xi)$, sandwiching another liquid $\epsilon_3(i\xi)$ and satisfying the condition $\epsilon_1(i\xi) < \epsilon_3(i\xi) < \epsilon_2(i\xi)$. For the case of two chiral slabs without substrate, the attractive contribution for large distances (i.e., for low frequencies) is smaller than that of semi-infinite chiral media due to the vacuum substrate, while the repulsive forces at short distances, that is, for high frequencies, almost do not depend on the thickness D; therefore, it is easier to obtain the repulsive force when the latter appears at short distances. Thus for the force between two chiral slabs with Drude metal substrate, because the repulsive contribution comes at very short distances, that is, for high frequencies, the finite-thickness slab does not influence the repulsive Casimir force too much until $D = 0.05\lambda_0$.

VI. CONCLUSION

In this paper, we used the extended Lifshitz theory to study the repulsive Casimir force between a semi-infinite Drude metal and a finite magnetic slab with or without substrate. For no substrate, we found that at large distances, the d dependence of the force is $1/d^5$; for the Drude metal substrate, an equilibrium point appears at intermediate distances. The thickness of the slab can tune the position of this equilibrium point. We also study the repulsive Casimir force between two identical chiral slabs, with and without substrate. For no substrate, we found that the finite slabs repel each other at short distances, while for large distances the d dependence of the attractive force is $1/d^6$. For the Drude metal substrate, we found that the finite thickness of the slab D does not influence the repulsive force at short distances too much until $D = 0.05\lambda_0$. These results are very useful to the experimentalists who are obliged to work with finite slabs.

ACKNOWLEDGMENTS

Work at Ames Laboratory was supported by the Department of Energy (Basic Energy Sciences) under Contract No. DE-AC02-07CH11358. R.Z. acknowledges the China Scholarship Council (CSC) for financial support.

[1] H. B. G. Casimir, Proc. K. Ned. Akad. Wet. **51**, 793 (1948).
[2] E. Buks and M. L. Roukes, Phys. Rev. B **63**, 033402 (2001).
[3] F. M. Serry, D. Walliser, and J. Maclay, J. Appl. Phys. **84**, 2501 (1998).
[4] I. E. Dzyaloshinskii, E. M. Lifshitz, and L. P. Pitaevskii, Adv. Phys. **10**, 165 (1961).
[5] J. N. Munday, F. Capasso, and V. A. Parsegian, Nature **457**, 170 (2009).
[6] A. W. Rodriguez, J. D. Joannopoulos, and S. G. Johnson, Phys. Rev. A **77**, 062107 (2008).
[7] T. H. Boyer, Phys. Rev. A **9**, 2078 (1974).
[8] O. Kenneth, I. Klich, A. Mann, and M. Revzen, Phys. Rev. Lett. **89**, 033001 (2002).
[9] U. Leonhardt and T. G. Philbin, New J. Phys. **9**, 254 (2007).
[10] R. Zhao, J. Zhou, Th. Koschny, E. N. Economou, and C. M. Soukoulis, Phys. Rev. Lett. **103**, 103602 (2009).
[11] R. Zhao, Th. Koschny, E. N. Economou, and C. M. Soukoulis, Phys. Rev. B **81**, 235126 (2010).
[12] F. S. S. Rosa, D. A. R. Dalvit, and P. W. Milonni, Phys. Rev. Lett. **100**, 183602 (2008),
[13] F. S. S. Rosa, D. A. R. Dalvit, and P. W. Milonni, Phys. Rev. A **78**, 032117 (2008).
[14] V. Yannopapas and N. V. Vitanov, Phys. Rev. Lett. **103**, 120401 (2009).
[15] D. R. Smith, J. B. Pendry, and M. C. K. Wiltshire, Science **305**, 788 (2004).
[16] C. M. Soukoulis, S. Linden, and M. Wegener, Science **315**, 47 (2007).
[17] C. M. Soukoulis, J. Zhou, Th. Koschny, M. Kafesaki, and E. N. Economou, J. Phys. Condens. Matter **20**, 304217 (2008).
[18] J. Valentine, S. Zhang, T. Zentgraf, E. Ulin-Avila, D. A. Genov, G. Bartal, and X. Zhang, Nature **455**, 376 (2008).
[19] E. M. Lifshitz, Sov. Phys. JETP **2**, 73 (1956).
[20] V. A. Parsegian and G. H. Weiss, J. Adhesion **3**, 259 (1972).
[21] Y. S. Barash, Radiophys. Quantum Electron. **21**, 1138 (1978).
[22] T. G. Philbin and U. Leonhardt, Phys. Rev. A **78**, 042107 (2008).
[23] A. Lambrecht, P. A. Maia Neto, and S. Reynaud, New J. Phys. **8**, 243 (2006).
[24] M. Born, E. Wolf, *Principles of Optics* (Cambridge Univ. Press, Cambridge, 1999).
[25] H. Cory and I. Rosenhouse, J. Mod. Opt. **39**, 1321 (1992).
[26] A. Lakhtakia, V. V. Varadan, and V. K. Varadan, J. Opt. Soc. Am. A **7**, 1654 (1990).
[27] S. J. Rahi, M. Kardar, and T. Emig, Phys. Rev. Lett. **105**, 070404 (2010).
[28] C. Raabe, L. Knöll, and D. Welsch, Phys. Rev. A **68**, 033810 (2003).
[29] A. P. McCauley, R. Zhao, M. T. H. Reid, A. W. Rodriguez, J. Zhou, F. S. S. Rosa, J. D. Joannopoulos, D. A. R. Dalvit, C. M. Soukoulis, and S. G. Johnson, Phys. Rev. B **82**, 165108 (2010).
[30] D. S. Dean, R. R. Horgan, A. Naji, and R. Podgornik, Phys. Rev. A **79**, 040101(R) (2009).